Evolutionnary autonomous VGSTV staircase climbing

Jean-Luc Paillat, Phillipe Lucidarme, Laurent Hardouin
jlpaillat@gmail.com, philippe.lucidarme@istia.univ-angers.fr
,laurent.hardouin@istia.univ-angers.fr

Laboratoire d'Ingénierie des Systèmes Automatisés (LISA), 62 Avenue Notre Dame du Lac - Angers - FRANCE

Abstract. This paper introduces an originally designed tracked robot. This robot belongs to the VGSTV (Variable Geometry Single Tracked Vehicle) category, which is actually a sub-group of Variable Geometry Vehicles well represented by the iRobot Packbot. Those robots have been used several times for search and rescue mission and seems to be a real asset because of their clearing capability. After a brief categorization, technical specification of our robot are presented and geometrical and dynamical models are computed in order to compare static and dynamic balance. Then, thanks to the results of the balance study, an autonomous staircase clearing controller based on artificial neural network is computed and tested. A general conclusion about possible improvements and future work ends the paper.

1 Introduction

UNMANNED GROUNDED VEHICLE (UGV) is a topically research field applied to a wide range of applications like for example exploration or missions in hostile environments. Research laboratories and robotics companies are currently working on the design of tele-operated and autonomous robots. According to [3] and [2] UGVs can be classified into three categories : Man-packable, Man-portable and Not man-portable.

The robots presented in this paper are classified in the man-packable and man-portable categories. In this class of robots, designers have to face the following dilemma : on one hand, build a small robot that can be easily carried and move into narrow environments. Unfortunately, it will generally result in poor obstacle clearing capability. On the other hand, build a bigger robot will increase its ability to surmount obstacles but will not enable the robot to go through narrow openings. The challenge is then to build a robot as small as possible with the higher obstacle clearing capability. Based on this observation the first part of this paper introduces the existing experimental and commercial robots and discusses about their clearing capabilities. The following of the paper describes an originally designed UGV (Fig. 3). This robot can be classified into the Variable Geometry Single Tracked Vehicle (VGSTV) category, i.e. it has the mechanical ability to modify its own shape according to the ground configuration. The design of our prototype is described in the third part with a

short discussion about the technical choices (information can be found on the project website : http://www.istia.univ-angers.fr/LISA/B2P2/b2p2.html). The next section introduces the dynamic model of the robot. The first tele-operated experiments have shown that the mass distribution is crucial to pass through large obstacles. Then, thanks to the results of the balance study, an autonomous staircase clearing controller based on artificial neural network is computed and tested. A general conclusion about possible improvements and future work ends the paper.

2 Existing UGVs

2.1 Wheeled and tracked vehicles with fixed shape

This category gathers non variable geometry robots (fig. 1a and b). Theoretically, this kind of vehicles are able to climb a maximum step twice less high than their wheel diameter. Therefore their dimensions are quite important to ensure a large clearing capability. This conception probably presents a high reliability [1] but those robots cannot be easily used in unstructured environments like after an earthquake [3].

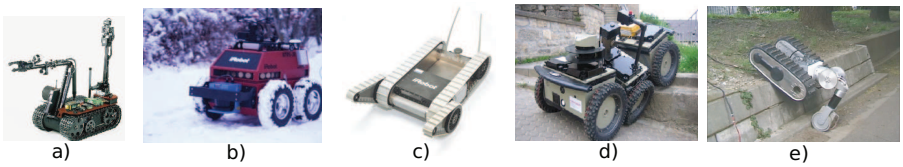

Fig. 1. a) : Talon-Hazmat robot (Manufacturer : Foster-Miller), b) : ATRV-Jr robot. Photo Courtesy of AASS, Örebro University c) : Packbot (manufacturer: IRobot), d) : RobuROC 6 (Manufacturer : Robosoft), e) : Helios VII

2.2 Variable Geometry Vehicle

A solution to ensure a large clearing capability and to reduce the dimensions consists in developing tracked vehicles which are able to modify their geometry in order to move their center of mass and climb higher obstacles than their wheel's diameters.

The Packbot robot (Fig. 1c) is probably one of the most famous commercial VGTV (Variable Geometry Tracked Vehicle). This robot is equipped with tracks and two actuated tracked flippers (372 mm long). The flippers are used to step over the obstacles. The obstacle clearing capability of this kind of VGTV depends on the size of the flippers. For more information and a detailed survey on clearance capability of the Packbot the reader can consult [6].

The robuROC6 (Fig. 1d) is equipped with 46.8 cm diameters wheels and can clear steps until 25cm (more than half the diameter of the wheels). Joints between the axles make this performance possible. An other original system called Helios VII (Fig 1e) [7] is equipped with an arm ended by a passive wheel which is able to elevate the chassis along a curb.

2.3 Variable geometry single tracked robots

Actually, there is a subgroup in VGTV called Variable Geometry Single-Tracked Vehicles (VGSTV) [13]. It gathers robots equiped with as tracks as propulsion motors. In most cases those robots are equipped with one or two tracks (one for each side). It can be divided into two groups :

- robots with deformable tracks,
- robots with non deformable tracks.

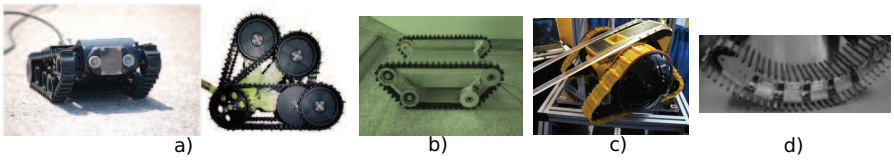

Fig. 2. a) : Micro VGTV (manufacturer: Inuktun Ltd) b) : VGSTV mechanism c) : Viper robot (Manufacturer : Galileo) d) : Rescue mobile track WORMY

Non-deformable tracks VGSTV The most famous example is the Micro VGTV. Illustrations of a prototype manufactured by the company Inuktun are presented on Fig. 2a. This robot is based on an actuated chassis used to modify the shape of the robot. The right picture of Fig. 2a shows the superimposing configurations. The tracks are kept tightened by a passive mechanism. The robot is thus equipped with three motors : two for the propulsion and one for the chassis joint.

Non commercial vehicles exists in the literature as the VGSTV mechanism (Fig. 2b) which is dedicated to staircase clearing. It is composed of two tracks and two articulations which allow it to have many symmetrical configurations such as a rectangle, trapezoids, inverse trapezoids etc.

Many other VGTV architecture exist, for further information reader can consult [19], [15], [4], [7] and [13].

Deformable tracks VGSTV Some single tracked robots have the ability to modify the flexing of their tracks. Two examples presented on Fig. 2 c and d, are able to adapt their shape to obstacles [12]. However, even if the control of

the robot seems easier with a flexible track than with a non flexible one, the mechanical conception could be more complicated.

According to the presented state of the art, for general purpose missions we beleive that the best compromise between design complexity, reliability, cost and clearing capabilities is the Variable geometry single tracked robots category. The next section will introduce and describe our prototype of VGSTV.

3 Prototype Description

The main interest of VGSTV (equipped with deformable tracks or not) is that it is practicable to overcome unexpected obstacles [13]. Indeed, thanks to the elastic property of the tracks the clearance of a rock in rough terrain will be more smoothly with a VGSTV (e. g. Fig 2) than with a VGTV (Fig. 1 c, d and e). On the Micro VGTV presented on Fig. 2, the tension of the tracks is mechanically linked with the chassis joint so it is constant during the movement. Nevertheless, in some cases, less tense tracks could increase the clearance capability by increasing the adherence. An interesting study about this point was developed by [8] giving a VGSTV able to climb staircases where the tension of the tracks was mechanically managed as on the MicroVGTV (Fig. 2a). However, this system was equipped with a spring to allow the tracks to adapt their shape to the ground (depending on the strength of the spring).

Fig. 3. B2P2 : clearing of a curb

The conception of our prototype is based on this previous work, but we decided to actuate the tension of the tracks. Indeed, by using two motors instead of one (Fig. 4) it is possible to increase the tracks adaptation to the ground developed by [8] and reach new configurations for the robot. As example, the solution proposed in this paper allows our robot to adopt classical postures of VGSTV (Fig. 3(a), 3(b) and 3(c)), but also other interesting positions. On Fig. 3 B2P2 is clearing a curb of 30 cm height with tense tracks. The position of the robot on Fig 3(c) can also be obtained with the Micro VGTV, but it is a non-safety position and B2P2 is close to topple over. On Fig. 3(d) the tracks have just been released. They take the shape of the curb and it can be cleared safely. This last configuration outlines the interest of using an active system instead

of a passive one. Consequently, although our prototype (Fig. 2b) belong to the VGSTV category and have not deformable tracks, it has the ability to adapt them to the ground (as deformable ones).
Besides, even if there is a risk of the tracks coming off, loosening the tracks may be an efficient mean of increase the surface in contact with the floor in rough terrain and then to improve the clearing capability of the structure. By the way, the risk could decreased by using sensor based systems to control the tension of the tracks or by modifying the mechanical structure of the robot (adding some kind of cramps on the tracks or using a guide to get back the tracks before it comes off).

3.1 Mechanical description

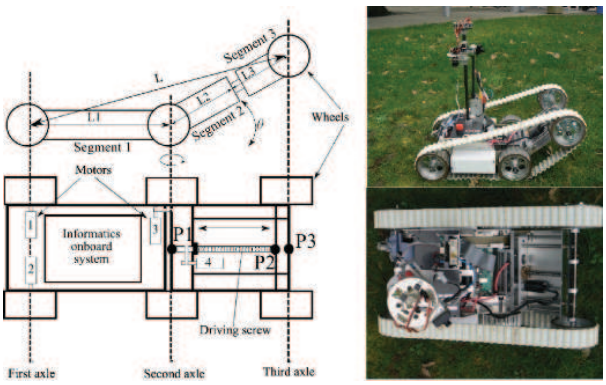

Fig. 4. Overview of the mechanical structure, side and top view of the real robot

This UGV is equipped with four motors. Fig. 4 presents the integration of the motors in the robot. Motors 1 and 2 are dedicated to the propulsion (tracks).
The actuated front part is composed of motors 3 and 4 :

- Motor 3 actuates the rotational joint, it allows the rotation of the front part around the second axle.
- Motor 4 actuates a driving screw, it controls the distance between the second axle and the third one.

To keep the tension of the tracks the trajectory of the third axle is given by an ellipse defined by two seats located on the first and the second axle.

$$L + (L_2 + L_3) = K \tag{1}$$

where the lengths L, L_2 and L_3 are referenced on Fig. 4. K is a constant parameter depending on the length of the tracks, L_3 evolves in order to achieve

equality (1) and is linked to the angle θ in the following manner :

$$L_3 = \frac{L_1^2 - K^2}{2(L_1 cos(\pi - \mid \theta \mid) - K)} - L_2 \tag{2}$$

4 Dynamic model

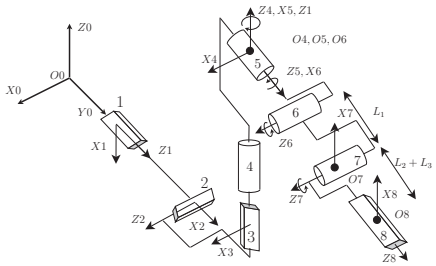

Fig. 5. B2P2's geometric model. Joints 1,2 and 3 represents the robot position. Joints 4, 5 and 6 symbolize respectively the yaw, roll and pitch, 7 and 8 are the actuated joints.

This section deals with the dynamic model of the robot which is based on the geometric model (Fig. 5) detailed on [17]. According to this model, the robot motion in a 3D frame (R_0) is described by the vector q of the 8 joints variables :

$$q = [q_1, q_2, q_3, q_4, q_5, q_6, q_7, q_8]^T$$

The dynamic model of a mechanical system establishes a relation between the effort applied on the system and its coordinates, generalized speeds and accelerations ([5] and [10]). In this section, the following notations are used :

- j describes the joints from 1 to 8,
- i describes the segments from 1 to 3 (referenced on Fig 4),
- n and m describes indexes from 1 to 8.

4.1 The Dynamic equations

The general dynamic equations of a mechanical system is :

$$\frac{d}{dt}\frac{\partial L}{\partial \dot{q_j}} - \frac{\partial L}{\partial q_j} = Q_j + T_j \tag{3}$$

- L is the Lagrangien of the system. It is composed of rigid segments, so there is no potential energy. Although the Lagrangien corresponds to the kinetic energy.
- q_j is the j^{th} joint variable of the system.

– Q_j is the gravity's torque applied to the j^{th} joint of the system.
– T_j is the external force's torque applied to the j^{th} joint of the system.

The kinetic energy is given by :

$$K = \sum_{i=1}^{n} \frac{1}{2} m_i v_i^T v_i + \frac{1}{2} w_i^T I_i w_i. \tag{4}$$

– m_i is the mass of the i^{th} element of the model,
– v_i is the linear speed of the i^{th} element's center of gravity,
– w_i is the angular speed of the i^{th} element's center of gravity,
– I_i is the matrix of inertia of the i^{th} element of the system.

In order to have homogeneous equations, w_i is defined in the same frame as I_i ; it allows to formulate v_i and w_i according to q :

$$v_i = J_{v_i}(q)\dot{q} \tag{5}$$

$$w_i = R_{0j}^T J_{w_i}(q)\dot{q} \tag{6}$$

where J_{v_i} and J_{w_i} are two matrices and R_{0j} is the transport matrix between the frame R_0 and the frame j linked to the segment i.

The kinetic energy formula is :

$$K = \frac{1}{2}\dot{q}^T \sum_i [m_i J_{v_i}(q)^T J_{v_i}(q) + J_{w_i}^T(q) R_{0j} I_i R_{0j}^T J_{w_i}(q)]\dot{q} \tag{7}$$

which can be rewritten as :

$$K = \frac{1}{2}\dot{q}^T D(q)\dot{q} \tag{8}$$

by developing the previous formula, we obtain :

$$K = \frac{1}{2} \sum_{m,n} d_{m,n}(q)\dot{q}_m\dot{q}_n \tag{9}$$

where $d_{m,n}(q)$ is the m, n^{th} element of the matrix $D(q)$.

The gravity's torque is given by :

$$Q_j = \sum_i g m_i \frac{\partial G_{zi}^0}{\partial q_j}. \tag{10}$$

– G_{zi}^0 is the z coordinate of the CoG of the i^{th} segment's computed in the base frame (R_0),
– g is the gravity acceleration.

Vector T (defined in (3)) is composed of the external forces' torque. For the robot presented here, there is no consideration of external forces, so the T vector only describes the motorized torques. Joints 1, 4, 7 and 8 are motorized, so the vector T is given by those four parameters. T_1 and T_4 are computed from the torques of motors 1 and 2 while T_7 and T_8 are deduced from motors 3 and 4.

The Euler-Lagrange equations can be written as :

$$\sum_m d_{jm}(q)\ddot{q}_m + \sum_{n,m} c_{nmj}(q)\dot{q}_n\dot{q}_m = Q_j + T_j \tag{11}$$

$$c_{nmj} = \frac{1}{2}[\frac{\partial d_{jm}}{\partial q_n} + \frac{\partial d_{jn}}{\partial q_m} - \frac{\partial d_{nm}}{\partial q_j}] \tag{12}$$

which is classically written as :

$$D(q)\ddot{q} + C(q,\dot{q})\dot{q} = Q + T \tag{13}$$

where $D(q)$ represents the matrix of inertia and $C(q,\dot{q})$ the centrifuge-coriolis matrix where X_{jm}, the jm^{th} element of this matrix, is defined as :

$$X_{jm} = \sum_n c_{nmj}\dot{q}_n.$$

Finally, the J_{vi} and J_{wi} matrix considered in (5) and (6) have to be computed.

4.2 J_{vi} and J_{wi} matrix formulation

The matrix which links articular speed and general speed of a segment is computed from the linear and angular speeds formulas. The goal is to find a matrix for each segment. They are composed of 8 vectors (one for each joint of the model).

The computation consists in formulating in the base frame, the speed ($V_{P_i}(j-1,j)^{R_0}$) of a point P_i given by a motion of the joint q_j attached to the frame j according to the frame $j-1$. Those parameters can be deduced from the law of composition speeds and the Denavitt Hartenberg (DH) formalism used for the geometric model [17]. Indeed, the general formulation is simplified by the geometric model. Only one degree of freedom (DoF) links two frames using the DH model and this DoF is a revolute or a prismatic joint. Moreover, the Z axis is always the rotation or translation axis, so the angular and linear speeds are given by four cases :

– The angular speed of a point for a revolute joint :

$$w_P(j-1,j)^{R_0} = R_{0,j}\begin{bmatrix}0\\0\\1\end{bmatrix}\dot{q}_j. \tag{14}$$

– The linear speed of a point for a revolute joint :

$$\begin{aligned} v_P(j-1,j)^{R_0} &= V_{O_j}^{R_{j-1}} + V_P^{R_j} + w_j \wedge O_j P^{R_j} \\ &= \quad \dot{q_j} R_{0,j} \begin{bmatrix} 0 \\ 0 \\ 1 \end{bmatrix} \wedge R_{0,j} P_j. \end{aligned} \tag{15}$$

– The angular speed of a point for a prismatic joint :

$$w_P(j-1,j) = \begin{bmatrix} 0 \\ 0 \\ 0 \end{bmatrix}. \tag{16}$$

– The linear speed of a point for a prismatic joint :

$$v_P(j-1,j)^{R_0} = R_{0,j} \begin{bmatrix} 0 \\ 0 \\ 1 \end{bmatrix} \dot{q_j} \tag{17}$$

where P_j is the P point's coordinates in R_j.
Thus, the matrix of a segment i is formulated by computing speeds for each joints as :

$$\begin{bmatrix} v_i \\ w_i \end{bmatrix} = J(q)\dot{q} = [J_{1,i}(q), J_{2,i}(q), ...J_{8,i}(q)]\, \dot{q} \tag{18}$$

where $J_{j,i}(q)$ is a vector which links the speed of the i^{th} segment according to the j^{th} joint. The first segment is not affected by the motion of joints 7 and 8 while the second is not affected by joint 8, therefore $J_{7,1}(q)$, $J_{8,1}(q)$ and $J_{8,2}(q)$ are represented by a null vector.

5 Balance criterion

The balance criterion used here are the ZMP (Zero Moment Point), widely used for the stability of humanoid robots and the Center of Gravity (CoG). Previous theoretical works and experiments have proved the ZMP efficiency [20]. It consists in keeping the point on the ground at which the moment generated by the reaction forces has no component around x and y axis ([11] and [9]) in the support polygon of the robot. When the ZMP is at the border of the support polygon the robot is teetering. Unlike the ground projection of the center of gravity, it takes into account the robot's inertia.

The purpose of the following is to defined the coordinates of this point in any frame of the model according to the configuration of the robot. The definition can be implemented into the Newton equations to obtain those coordinates. In any point of the model : $M_0 = M_z + OZ \wedge R$ (M_0 and M_z define respectively the moment generated by the reaction force R at the points 0 and z).
According to the previous definition, there is no moment generated by reaction

forces at the Zero Moment Point. Consequently, if Z defines the ZMP coordinates $M_0 = OZ \wedge R$. This formulation can be implemented into the Newton equations as :

$$\delta_0 = M_0 + \boldsymbol{OG} \wedge \boldsymbol{P} + \boldsymbol{OG} \wedge \boldsymbol{F_i} \tag{19}$$

where P is the gravity force, G is the robot's center of gravity and F_i is the inertial force (the first Newton's law gives $F_i = -m\ddot{G}$). According to the ZMP definition, the equation (19) can be formulated as :

$$\delta_0 = \boldsymbol{OZ} \wedge \boldsymbol{R} + \boldsymbol{OG} \wedge \boldsymbol{P} + \boldsymbol{OG} \wedge \boldsymbol{F_i} \tag{20}$$

$$\begin{cases} \delta_{0x} = Z_y R_z + G_y P_z - G_z P_y - G_z F i_y \\ \delta_{0y} = -Z_x R_z + G_z P_x - G_x P_z \end{cases} \tag{21}$$

$$\begin{cases} Z_y = \frac{\delta_{0x} - G_y P_z + G_z P_y + G_z F i_y}{R_z} \\ Z_x = \frac{-\delta_{0y} + G_z P_x - G_x P_z}{R_z}. \end{cases} \tag{22}$$

Also, it is possible to compute the position of the ZMP as a function of q (δ_0 depends on the matrix $D(q)$).

Assuming the ground knowledge, the ZMP computation gives a criterion to determinate the stability of the platform.

6 Results

This section presents the numerical computation of the criterion in the case of the clearance of a staircase (staircase set of 15 cm risers and 28 cm runs) with an average speed of 0.13 $m.s^{-1}$. The robot is equipped with a 2-axis inclination sensor that provides rolling and pitching. Vector q entries are measured using encoders on each actuated axis of the robot. Data have been stored during the experiments and the models (CoG and ZMP) have been computed off-line. This computation does not take into account the tracks' weight which is negligible in regard with the robot's weight. Fig. 6 presents the evolution of the ZMP (left) and the difference between those two criterion (right) during all the clearance. P_1 P_2 and P_3 represents the z-coordinates in the frame R_5 (Fig. 5) of three points of the robot which localization are noticed on Fig. 4.

This experiment allows us to validate the presented model and confirms the computation of the ZMP criterion. However, as it is shown on Fig. 6, the average difference between the ZMP and the COG is insignificant (about 0.21%). Moreover, the two peaks (A and B) on the Fig. 6 are not due to the dynamics of the system but to measurement errors. As the acceleration is measured with the encoders (linked to the motor shaft), when the tracks slip, the measurement is erroneous. The ZMP is computationally more expensive, needs more sensor measurements and the difference with the CoG is negligible. For these reasons,

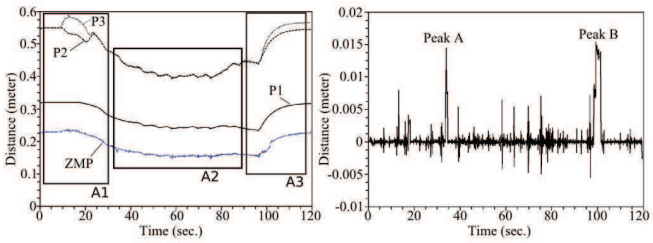

Fig. 6. Experiment's results. The left chart represents the evolution of the ZMP and the right one, the difference between CoG and ZMP.

we conclude that the CoG seems well suited for this kind of experiments. Anyway, in the case where fast obstacle clearance may be necessary, the CoG may not longer be considered and the ZMP must be used instead.

7 Autonomous stair climbing controller

The purpose of the following is to present a reactive autonomous staircase climbing controller. This study was performed through a home made C++ software which simulates the behavior of a VGTV in staircase climbing situations. The simulator is based on the model of our prototype B2P2. Giving the reduced impact of dynamics effects on the robot as explained previously, the CoG is considered as balance criterion in the simulations. The system presented here consists in controlling the elevation of the front part (e.g. the shape of the robot and implicitly the position of CoG).Currently, the tension of the tracks is controlled by a man-programmed algorithm that automatically adapts the shape of the robot according to ground.

7.1 Entries of the system

The system has to be able to react differently in regards with the climbing stage. So, entries have to differ according to the stage (first step, middle steps, final step). The chassis inclination measurement allows to check out the first stage (if the ground is plane) but does not help to conclude about the two others stages (Fig. 7). On the other hand, a distance sensor could check out the last stage as it is shown on Fig. 7. So considering that the robot is always parallel to the step in front of it, the inclination and distance sensors could be sufficient to achieve an autonomous staircase climbing.

7.2 Controller

As explained by [16] genetic algorithms can be used to train and optimize control systems. Typically, Artificial Neural Networks (ANNs) are often used as control systems for obstacle avoidance or grasping tasks ([14]) because such controller

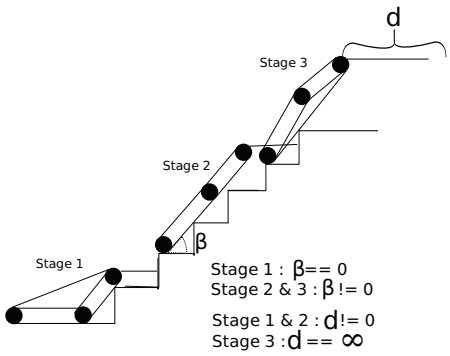

Fig. 7. Stage decomposition during climbing

can approximate a wide range of mathematical functions. An ANN is composed of several units linked by weighted connections w_{ij}. Each unit i has entries x_j and one output y_i which is a function $\sigma()$ of $\sum_j^N (w_{ij}.x_j)$ where w_{ij} corresponds to the weight of the link between two neurones. Theoretically, neurones are organized in layers to perform a neural network. This network can be feed-forward (signal travel from inputs units forward to output units) or recurrent (there may be feedback connections from neuron in upper layer or in the same layer). As introduced, in the case of autonomous staircase climbing with a VGSTV as B2P2, the system have to control the elevation of the front part according to the position of the robot in the staircase. Otherwise, the output of the network is the elevation of the front part. Consequently the neural network architecture chosen is a feed-forward network with one hidden layer (Fig. 8) that must be addressed to approximate non linear functions. Indeed, a recurrent network does not seem useful, because a variation of the output (elevation angle) includes a variation of the network entries (IR distance sensors and inclination sensor).

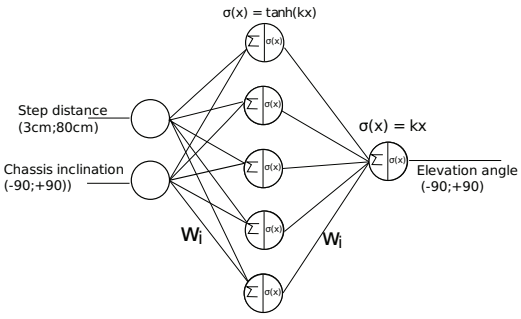

Fig. 8. Neural Network Model

7.3 Evolutionnary training

In the controller, all the parameters are known except the 15 synaptic weights (w_i) which are deduced by an evolutionary algorithm based on a classical genetic approach. As the structure of the network has been fixed, only those weights have to be optimized. Consequently, a chromosome is only composed of the weights W_i.

w_1	w_2	...	w_i	...	w_{14}	w_{15}

Table 1. Chromosome description

Selective reproduction Each generation is composed of 200 sets of chromosomes composed of fifteen parameters randomly selected into $[-1, 1]$. After each generation, a selective reproduction is performed in order to compute the next generation. Here this selection is roulette wheel based that allow the best individual to be statistically selected more frequently. Otherwise :

$$p_i = \frac{f_i}{\sum_i^N f_i}$$

Where p_i is the probability of selection for the individual i, f_i stands for the fitness of the individual i and N represents the number of individual in the previous generation.

A selection process is performed for each chromosome element (e. g. fifteen times) to compute the next generation. However, the best individual of each generation is duplicated for the next generation without selective reproduction. Additionally, a mutation process is performed by replacing by a random value in the range $[-1, 1]$ a randomly selected gene (chromosome element) for 10% of the new generation to prevent premature convergence.

Fitness Function As the goal is to climb staircases, the fitness function must be linked to the number of steps cleared. As this parameter is discrete, we combined it with another parameter that minimizes the energy (directly linked to the elevation part movement). Moreover, minimizing the energy provides smooth trajectory of the robot. It is expressed as follow :

$$f_i = \frac{N_{steps}}{E}$$

Where f_i is the fitness of the individual i, N_{steps} stands for the number of steps cleared by individual i and E represents parameter depending on the average speed of the front part (V) as :

$$E = \begin{cases} 1 & \text{if } V < \text{threshold} \\ V & \text{otherwise} \end{cases}$$

7.4 results

The simulation was performed with a classical staircase sets of five steps of 15 cm risers and 25 cm runs. Fifty generations was tested in order to have a characteristic convergence (Fig. 9(a)). Simulation results are shown on Fig. 9(b)

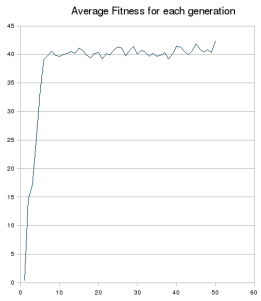

(a) Generation convergence

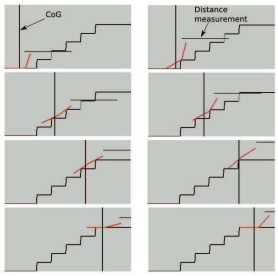

(b) Staircase climbing simulation results

Step length (cm) \ Step height (cm)	15	20	25	30
15	100%	100%	100%	100%
20	60%	80%	100%	100%

(c) Controller performance table

Fig. 9. Results

In order to evaluate how generic are the produced results, the best individual has to get over several kind of staircases as described in table 9(c). The percentage of cleared steps is indicated according to the length and the height of the steps. Note that the 25 cm is the maximum step height that the prototype is able to clear in tele-operated staircase clearance.

The controller seems to be able to perform an autonomous staircase clearing in regard with the quality of information given by the environment.

Conclusion

This paper presents a way to climb staircases autonomously with classical VGTVs by using their ability to modify their geometry in order to adapt themselves to the ground. It consists in a neural network which compute the elevation of the robot's front part in respect to its inclination and the distance between it and the next step. However, it was necessary to study the behavior of our robot in order to validate robot's model in context of a staircase clearance. Those simulation results have been implemented on our prototype B2P2 ; A video of autonomous staircase climbing can be found at http://www.istia.univ-angers.fr/LISA/B2P2/b2p2.html. Some improvement should be done to increase the reliability but those first result seems promising. Our future works focuses on a survey about control of VGSTV equipped with n-degrees of freedom using interval analysis in order to maximize the adaptability of such robots.

References

1. Carlson, J., Murphy, R.R.: Reliability analysis of mobile robots. International Conferenee on Robotics and Automation (September 2003)
2. Carlson, J., Murphy, R.R.: How ugvs physically fail in the field. IEEE Transactions on robotics 21(3), 423–437 (June 2005)
3. Casper, J., Murphy, R.R.: Human-robot interactions during the robot-assisted urban search and rescue response at the world trade center. IEEE Transactions on systems, man, and cybernetics 33(3), 367–384 (June 2003)
4. Clement, G., Villedieu, E.: Variable geometry track vehicle. Us patent (1987)
5. Craig, J.J.: Introduction to Robotics Mechanics and control. Silma, 2 edn. (1989)
6. Frost, T., Norman, C., Pratt, S., Yamauchi, B.: Derived performance metrics and measurements compared to field experience for the packbot. Proceedings of the 2002 PerMIS Workshop (2002)
7. Guarnieri, M., Debenest, P., Inoh, T., Fukushima, E., Hirose, S.: Development of helios vii : an arm-equipped tracked vehicle for search and rescue operations. IEEE/RSJ Int. Conference on Intelligent Robots (2004)
8. Iwamoto, T., Yamamoto, H.: Variable configuration track laying vehicle (us patent) (March 1983)
9. Kajita, S., Kanehiro, F., Kaneko, K., Fujiwara, K., Harada, K., Yokoi, K., Hirukawa, H.: Biped walking pattern generation by using preview control of zero moment point. Proceedings of the 2002 IEEE Internationnal Conference on Robotics ans Automation (September 2003)
10. Khalil, W., Dombre, E.: Modeling, Identification and Control of Robots. Kogan Page Science, 2 edn. (2004)
11. Kim, J., Chung, W.K., Youm, Y., Lee, B.H.: Real time zmp compensation method using null motion for mobile manipulators. Proceedings of the 2002 IEEE Internationnal Conference on Robotics ans Automation (May 2002)
12. Kinugasa, T., Otani, Y., Haji, T., Yoshida, K., Osuka, K., Amano, H.: A proposal of flexible mono-tread mobile track. Internationnal Conference on Intelligent Robots and Systems (Sept 2008)
13. Kyun, L.S., Il, P.D., Keun, K.Y., Byung-Soo, K., Sang-Won, J.: Variable geometry single-tracked mechanism for a rescue robot. IEEE International Workshop on Safety, Security and Rescue Robotics pp. 111–115 (2005)
14. Lucidarme, P.: Evolution of a mobile robot's neurocontroller on the grasping task. Internationnal Conference on Informatics in Control, Automation and Robotics (2008)
15. Misawa, R.: Stair-climbing crawler transporter. Us patent (1997)
16. Nolfi, S., Floreano, D.: Evolutionnary Robotics. The MIT Press (2000)
17. Paillat, J.L., Lucidarme, P., Hardouin, L.: Variable geometry tracked vehicle, description, model and behavior. Conference Mecatronics (May 2008)
18. Sliwka, J., Jaulin, L.: Robust localization for an easier tele-operation. Conference on Humans Operating Unmanned Systems (September 2008)
19. Vincent, I., Trentini, M.: Shape-shifting tracked robotic vehicle for complex terrain navigation: Characteristics and architecture. Technical memorandum, Defence R and D Canada (December 2007)
20. Vukobratovic, M., Borovac, B.: Zero-momment point - thirty five years of its life. Internationnal journal of humanoid Robotics 1(1), 157–173 (2004)